WILEY-VCH

Supporting Information for

# Flexible spin orientation optimized lower-density zero thermal expansion in the Sc-based kagome magnets

*Haowei Zhou,[1,#] Yanming Sun,[1,#] Yili Cao,[1,*] Sergii Khmelevskyi,[2] Tieqiao Zhang,[3] Yaozu Shen[1], Zhao Pan,[4] Kun Lin,[1] Maxim Avdeev,[5,6] and Xianran Xing[1,*]*

H. Zhou, Y. Sun, Y. Cao, K. Lin, X. Xing

Institute of Solid State Chemistry

State Key Laboratory for Advanced Metals and Materials

University of Science and Technology Beijing

Beijing 100083, P.R. China

Emails: yilicao@ustb.edu.cn; xing@ustb.edu.cn

S. Khmelevskyi

Vienna Scientific Cluster Research Center

Technical University of Vienna

Operngasse 10, Vienna A-1040 , Austria

T. Zhang

School of Materials Science and Engineering

Tsinghua University

Beijing 100084, P.R. China

Z. Pan

Beijing National Laboratory for Condensed Matter Physics

Institute of Physics, Chinese Academy of Sciences

Beijing 100190, P.R. China

*M. Avdeev*

Australian Nuclear Science and Technology Organisation

Lucas Heights, New South Wales 2234, Australia

School of Chemistry

The University of Sydney

Sydney, New South Wales 2006, Australia

## Supporting figures and discussions

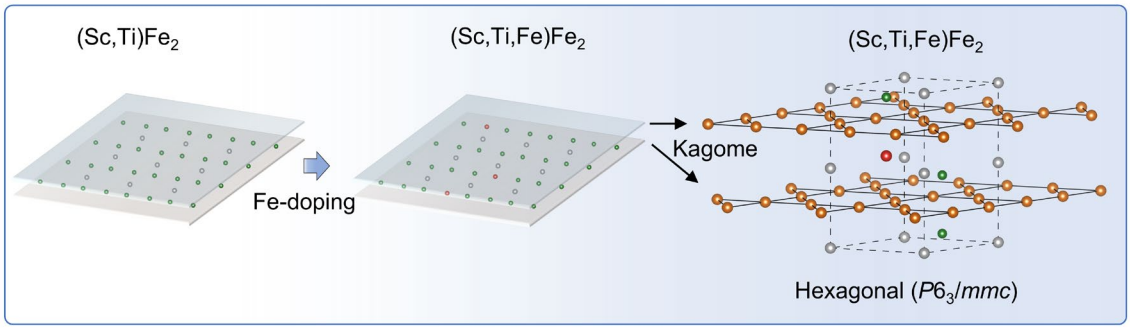


**Figure S1.** The schematic of the hexagonal structure of Fe doping in (Sc,Ti)$Fe_2$.

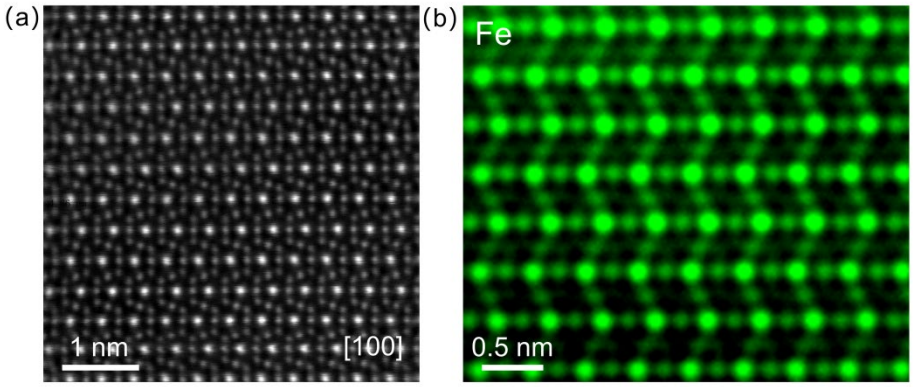


**Figure S2.** (a) HAADF-STEM image along the [100] zone axis of $y$ = 0.4; (b) Atomically resolved energy-dispersive X-ray spectroscopy (EDXS) mappings Fe elements.

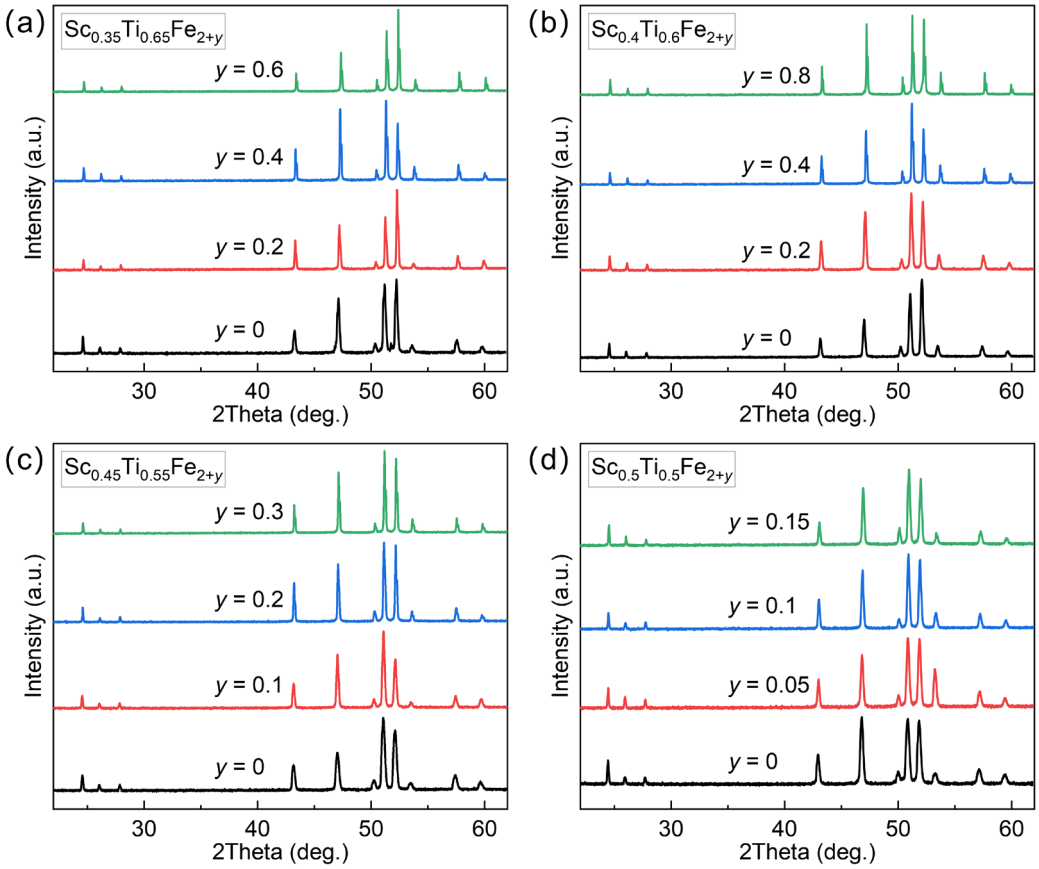


**Figure S3.** XRD patterns of (a) $Sc_{0.35}Ti_{0.65}Fe_{2+y}$, (b) $Sc_{0.4}Ti_{0.6}Fe_{2+y}$, (c) $Sc_{0.45}Ti_{0.55}Fe_{2+y}$ and (d) $Sc_{0.5}Ti_{0.5}Fe_{2+y}$ annealed at 1473 K under Co Kα radiation.

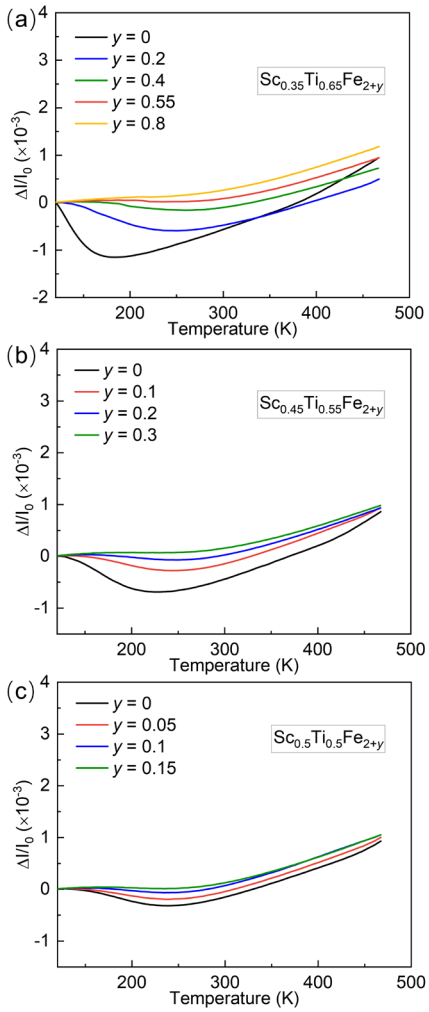


**Figure S4.** Linear thermal expansion ($\Delta I/I_0$) for (a) $Sc_{0.35}Ti_{0.65}Fe_{2+y}$ and (b) $Sc_{0.45}Ti_{0.55}Fe_{2+y}$ and (c) $Sc_{0.5}Ti_{0.5}Fe_{2+y}$.

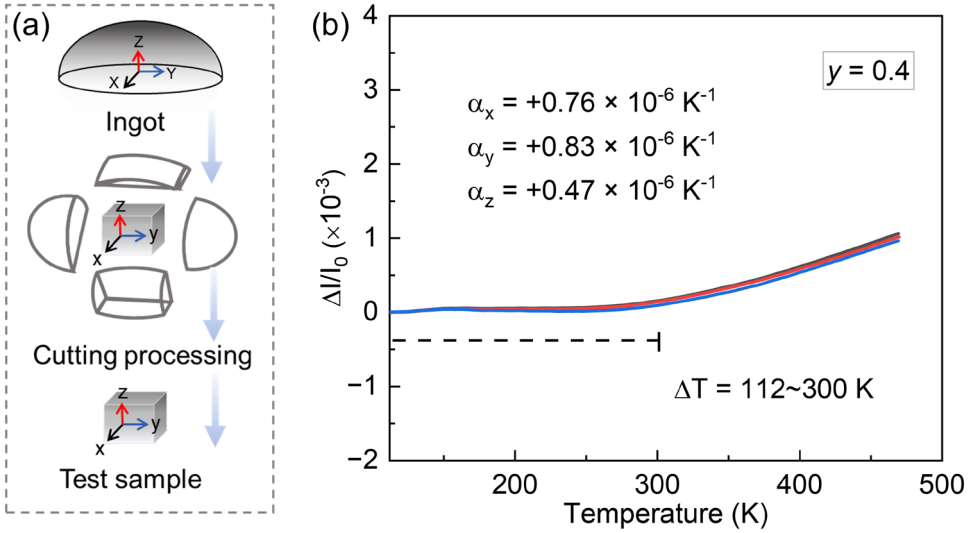


**Figure S5.** (a) Schematic diagram of test sample processing. (b) Linear thermal expansions of $y = 0.4$ along three apparent orientations of the anothor ingot.

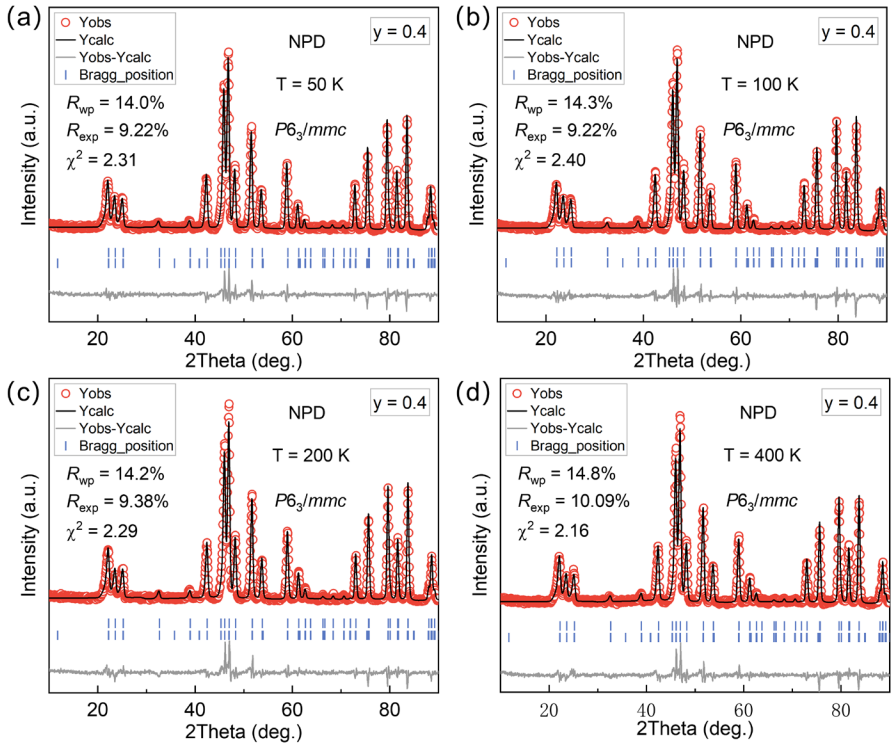


**Figure S6.** Neutron powder diffraction refinement of the hexagonal $y = 0.4$ at 50 K, 100 K, 200 K and 400 K.

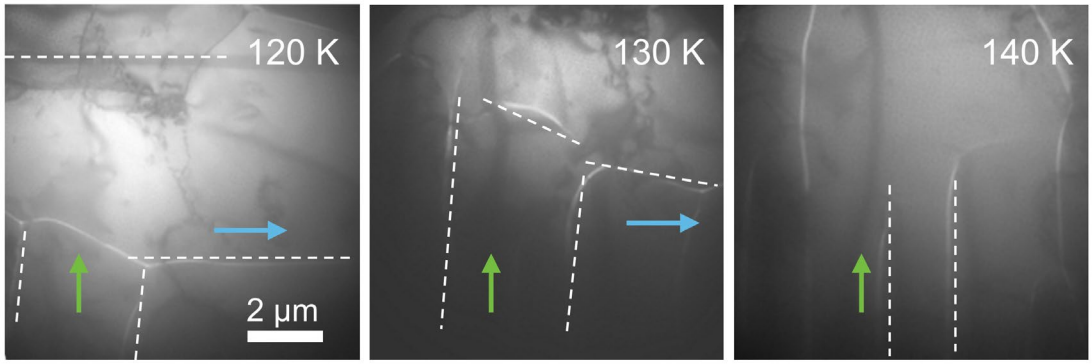


**Figure S7.** L-TEM images of the evolution of the magnetic domains of $y = 0$ as a function of temperature at zero magnetic fields.

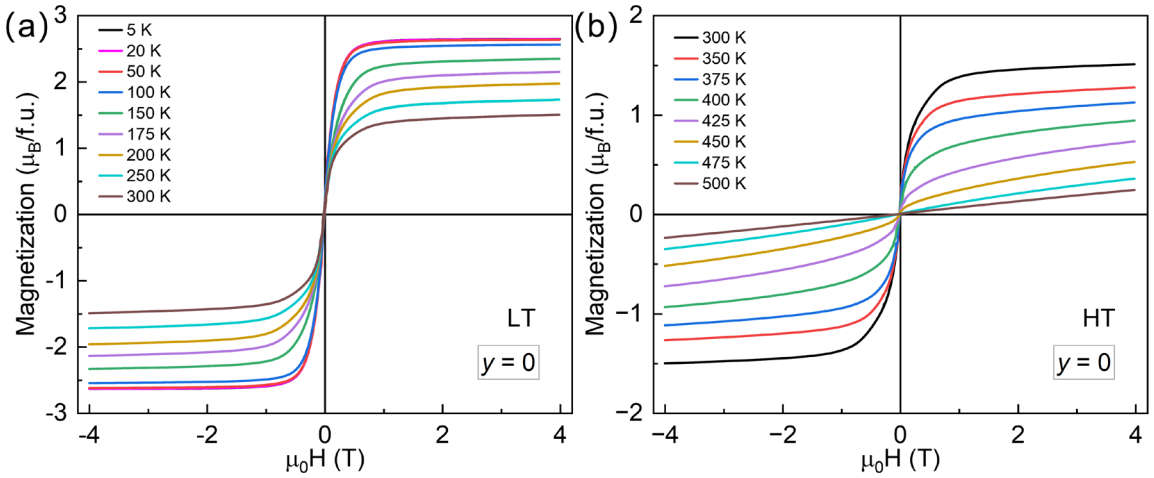


**Figure S8.** Isothermal *M*-*H* curves (-4−4 T) at (a) 5−300 K and (b) 300−500 K for $Sc_{0.4}Ti_{0.6}Fe_2$ (denoted as $y = 0$).

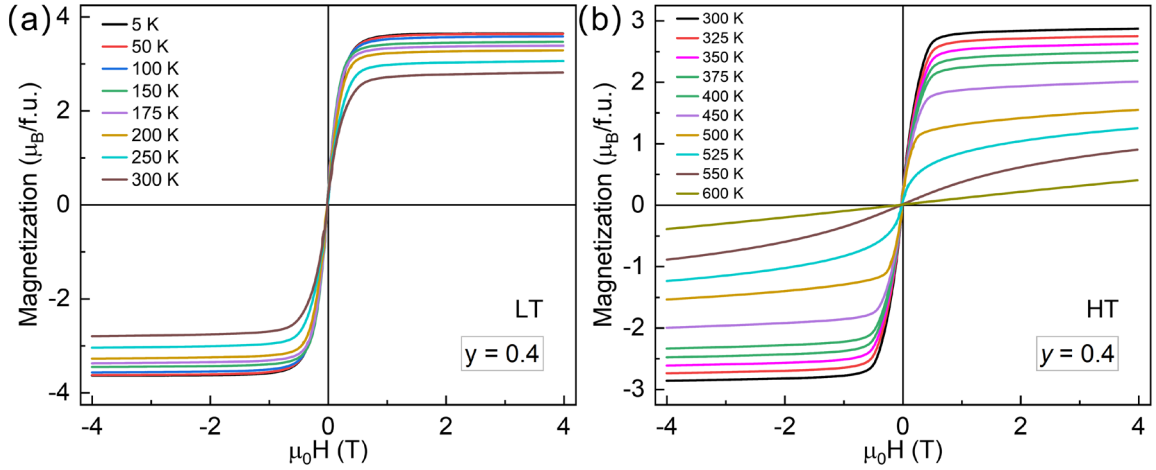


**Figure S9.** Isothermal *M*-*H* curves (-4−4 T) at (a) 5−300 K and (b) 300−600 K for $Sc_{0.4}Ti_{0.6}Fe_{2.4}$ (denoted as $y = 0.4$).

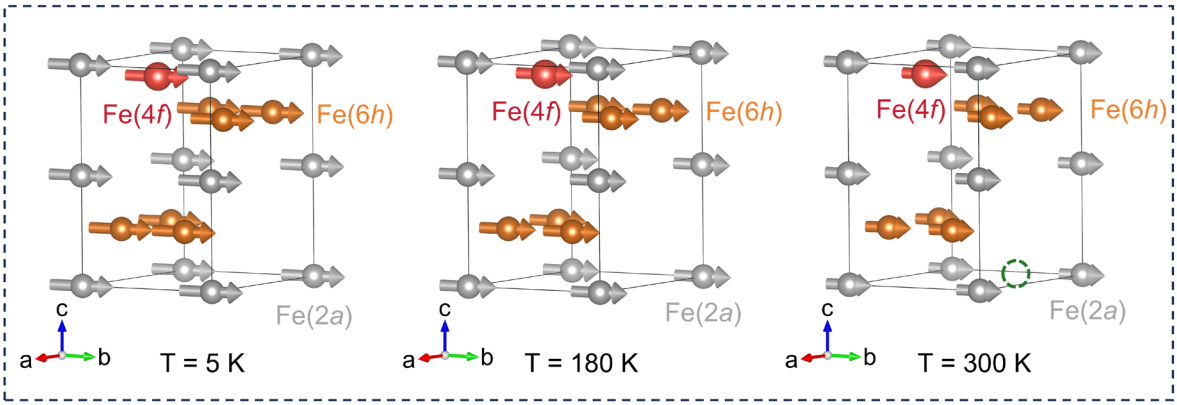


**Figure S10.** The average magnetic structure of y = 0.4 at 5 K, 180 K and 300 K, respectively, the magnetic moments of Fe(2*a*) and Fe(6*h*) were obtained from NPD refinements, while the occupancy of Fe(4*f*) was confirmed jointly by STEM-EDX and Mössbauer spectroscopy. By integrating all experimental results, the magnetic structure shown in the figure was constructed.

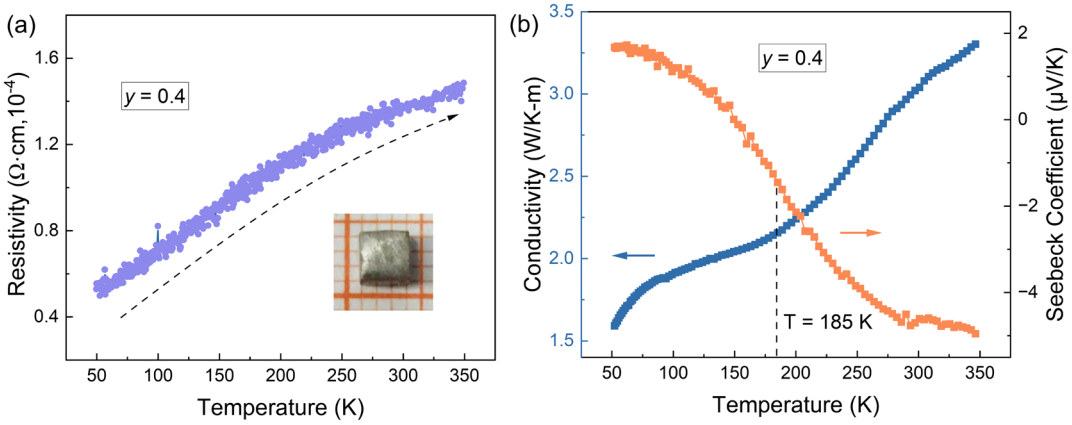


**Figure S11.** (a) Temperature dependence of resistivity for $y = 0.4$ with the insets of test sample; (b) Temperature dependence of conductivity and seebeck coefficient for $y = 0.4$

**Table S1**. Summary of density, operating temperature window, coefficient of thermal expansion (αl/αV), magnetization, and compositional cost of the ZTE metals.

| ZTE alloy | Density ($g/cm^3$) | Operating Temperature (K) | CTE ($\times 10^{-6}$ $K^{-1}$) | Ms (emu/g) | Cost[(a)] (CNY/kg) | Refer. |
|---|---|---|---|---|---|---|
| $Hf_{0.8}Nb_{0.2}Fe_{2.5}$ | 10.1 | 5-460 | $\alpha_l = 1.07$ | 73.7 (T = 5 K) | 9606 | 1 |
| $TbCo_{1.9}Fe_{0.1}$ | 9.76 | 123-307 | $\alpha_l = 0.48$ | - | 10961 | 2 |
| $Hf_{0.6}Ti_{0.4}Fe_{2.5}$ | 9.12 | 10-480 | $\alpha_V = 1.7$ | 91.6 (T = 25 K) | 8270 | 3 |
| $Zr_{0.7}Ta_{0.3}Fe_2$ | 8.91 | 10-430 | $\alpha_l = 0.9$ | 75.2 (T = 5 K) | 2226 | 4 |
| $Zr_{0.8}Ta_{0.2}Fe_{1.7}Co_{0.3}$ | 8.54 | 5-360 | $\alpha_l = 0.21$ | 72.3 (T = 5 K) | 2005 | 5 |
| $Fe_{65}Ni_{35}$ | 8.12 | 193-373 | 1.5 | - | 455 | 6 |
| $Fe_{63}Ni_{32}Co_5$ | 8.07 | 218-368 | $\alpha_l = 0.63$ | - | 508 | 7 |
| $Er_2Fe_{19}B_{1.35}$ | 7.91 | 100-550 | $\alpha_l = 0.28$ | 99.6 (T = 10 K) | 1517 | 8 |
| $(Zr_{0.65}Nb_{0.35})_{0.95}Fe_{0.05}Fe_2$ | 7.85 | 4-425 | $\alpha_l = 0.47$ | 103 (T = 5 K) | 991 | 9 |
| $Zr_{0.8}Nb_{0.2}Fe_2$ | 7.83 | 3-470 | $\alpha_l = 1.4$ | - | 1108 | 10 |
| $Zr_{0.75}Nb_{0.25}Fe_2Co_{0.1}$ | 7.81 | 3-440 | $\alpha_l = 1.07$ | 85.4 (T = 5 K) | 1090 | 11 |
| $Sc_{0.4}Ti_{0.6}Fe_{2.4}$ | 6.56 | 5-300 | $\alpha_V = 1.93$ | 112.8 (T = 5 K) | 4172 | This work |

[(a)] The unit price of raw materials is based on the 2025 price data provided by Zhongnuo New Materials (Beijing) Technology Company, Limited. The calculation procedure is as follows: first, the atomic weights, metal prices, and chemical formula are prepared; then, the molar fraction of each element is calculated and converted into the mass fraction; finally, the mass fraction is multiplied by the corresponding metal unit price to estimate the sample cost.

**Table S2.** Final refined structural parameters for hexagonal $Sc_{0.4}Ti_{0.6}Fe_{2.4}$ (denoted as $y = 0.4$) by neutron powder diffraction at 5 K.

| Atom | Site | *x*, *y*, *z* | Occupancy |
|---|---|---|---|
| Sc | 4*f* | 0.33333, 0.66667, 0.06335 | 0.53 |
| Ti | 4*f* | 0.33333, 0.66667, 0.06335 | 0.35 |
| Fe | 4*f* | 0.33333, 0.66667, 0.06335 | 0.12 |
| Fe | 2*a* | 0,0,0 | 1 |
| Fe | *6h* | 0.83036, 0.66062, 0.25000 | 1 |

* $a = b = 4.85822(2)$ Å, $c = 7.92112(3)$ Å and $V = 161.909(1)$ Å$^3$, space group: $P6_3/mmc$, $R_{wp}$ ~ 14.2%; $\chi^2$ ~ 2.4.

**Table S3.** Temperature dependence of lattice parameters by NPD patterns for $y = 0.4$.

| Temperature (K) | a (Å) | c (Å) | unit cell volume (Å$^3$) |
|---|---|---|---|
| 5 | 4.85822(2) | 7.92112(3) | 161.909(1) |
| 10 | 4.85828(2) | 7.92118(3) | 161.915(1) |
| 20 | 4.85822(2) | 7.92099(3) | 161.907(1) |
| 30 | 4.85817(2) | 7.92104(3) | 161.904(1) |
| 40 | 4.85821(2) | 7.92118(3) | 161.910(1) |
| 50 | 4.85819(2) | 7.92109(3) | 161.907(1) |
| 60 | 4.85816(2) | 7.92112(3) | 161.905(1) |
| 70 | 4.85818(2) | 7.92125(3) | 161.909(1) |
| 80 | 4.85818(2) | 7.92138(3) | 161.912(1) |
| 90 | 4.85822(2) | 7.92171(3) | 161.921(1) |
| 100 | 4.85835(2) | 7.92187(3) | 161.933(1) |
| 110 | 4.85833(2) | 7.92203(3) | 161.935(1) |
| 120 | 4.85834(2) | 7.92223(3) | 161.940(1) |
| 130 | 4.85839(2) | 7.92239(3) | 161.947(1) |
| 140 | 4.85842(2) | 7.92284(3) | 161.958(1) |
| 150 | 4.85834(2) | 7.92270(3) | 161.949(1) |
| 160 | 4.85839(2) | 7.92323(3) | 161.964(1) |
| 170 | 4.85836(2) | 7.92336(3) | 161.964(1) |
| 180 | 4.85818(2) | 7.92361(4) | 161.958(1) |
| 190 | 4.85818(2) | 7.92366(3) | 161.958(1) |
| 200 | 4.85818(2) | 7.92400(3) | 161.965(1) |
| 210 | 4.85811(2) | 7.92408(4) | 161.962(1) |
| 220 | 4.85808(2) | 7.92411(3) | 161.961(1) |
| 230 | 4.85804(2) | 7.92433(4) | 161.963(1) |
| 240 | 4.85799(2) | 7.92432(4) | 161.959(1) |
| 250 | 4.85798(2) | 7.92449(4) | 161.962(1) |
| 260 | 4.85802(2) | 7.92493(4) | 161.974(1) |
| 270 | 4.85805(2) | 7.92484(4) | 161.974(1) |
| 280 | 4.85805(2) | 7.92517(4) | 161.981(1) |
| 290 | 4.85815(2) | 7.92539(4) | 161.992(1) |
| 300 | 4.85823(2) | 7.92581(4) | 162.006(1) |
| 310 | 4.85833(2) | 7.92598(4) | 162.016(1) |
| 320 | 4.85847(2) | 7.92629(4) | 162.031(1) |
| 330 | 4.85858(2) | 7.92679(4) | 162.049(1) |
| 340 | 4.85883(2) | 7.92702(4) | 162.070(1) |
| 350 | 4.85899(2) | 7.92764(4) | 162.094(1) |
| 375 | 4.85941(2) | 7.92871(4) | 162.143(1) |
| 400 | 4.85999(2) | 7.92964(4) | 162.202(1) |
| 450 | 4.86093(2) | 7.93171(4) | 162.307(1) |
| 500 | 4.86231(2) | 7.93467(5) | 162.460(1) |
| 525 | 4.86299(2) | 7.93578(5) | 162.528(1) |
| 550 | 4.86371(2) | 7.93726(5) | 162.606(1) |

**Table S4.** Temperature dependence of moments by NPD patterns for hexagonal $y = 0.4$.

| Temperature (K) | 2a ($\mu_B$) | 6h ($\mu_B$) |
|---|---|---|
| 5 | 2.81(9) | 2.70(5) |
| 10 | 2.77(9) | 2.66 |
| 20 | 2.76(9) | 2.66(5) |
| 30 | 2.69(9) | 2.58(5) |
| 40 | 2.88(9) | 2.72(5) |
| 50 | 2.88(9) | 2.62(5) |
| 60 | 2.85(9) | 2.69(5) |
| 70 | 2.90(10) | 2.61(5) |
| 80 | 2.85(9) | 2.81(5) |
| 90 | 2.80(9) | 2.58(5) |
| 100 | 2.73(9) | 2.61(5) |
| 110 | 2.84(9) | 2.78(5) |
| 120 | 2.85(9) | 2.69(5) |
| 130 | 2.98(9) | 2.83(5) |
| 140 | 2.99(9) | 2.80(6) |
| 150 | 2.92(9) | 2.77(6) |
| 160 | 3.05(9) | 2.72(6) |
| 170 | 3.29(9) | 2.77(6) |
| 180 | 3.26(9) | 2.67(6) |
| 190 | 3.09(9) | 2.41(6) |
| 200 | 3.11(9) | 2.45(6) |
| 210 | 3.18(10) | 2.63(7) |
| 220 | 3.19(10) | 2.53(8) |
| 230 | 2.98(10) | 2.43(8) |
| 240 | 2.89(10) | 2.35(8) |
| 250 | 3.14(10) | 2.45(8) |
| 260 | 3.00(10) | 2.49(8) |
| 270 | 3.05(10) | 2.46(8) |
| 280 | 3.00(10) | 2.38(8) |
| 290 | 2.81(11) | 2.28(8) |
| 300 | 2.90(10) | 2.25(8) |
| 310 | 2.65(11) | 2.11(8) |
| 320 | 2.58(11) | 2.04(8) |
| 330 | 2.69(11) | 2.14(8) |
| 340 | 2.73(10) | 2.14(8) |
| 350 | 2.78(10) | 2.28(8) |
| 375 | 2.57(11) | 2.03(9) |
| 400 | 2.48(11) | 2.07(8) |
| 450 | 2.36(12) | 1.90(9) |
| 500 | 1.33(20) | 1.24(12) |
| 525 | 0 | 0 |
| 550 | 0 | 0 |

**Table S5.** Summary of full Rietveld statistics of NPD of y = 0.4, including $R_{wp}$, $R_{mag}$, and $\chi^2$.

| Temperature (K) | $R_{wp}$ (%) | $R_{mag}$ (%) | goodness of fit $\chi^2$ |
|---|---|---|---|
| 5 | 14.1 | 3.18 | 2.36 |
| 10 | 14.0 | 4.58 | 2.31 |
| 20 | 14.7 | 3.83 | 2.44 |
| 30 | 14.3 | 3.79 | 2.26 |
| 40 | 14.4 | 3.29 | 2.31 |
| 50 | 14.0 | 2.88 | 2.31 |
| 60 | 14.5 | 4.59 | 2.51 |
| 70 | 13.9 | 3.25 | 2.30 |
| 80 | 14.0 | 3.33 | 2.33 |
| 90 | 14.0 | 2.94 | 2.29 |
| 100 | 14.3 | 4.33 | 2.40 |
| 110 | 13.9 | 4.13 | 2.25 |
| 120 | 13.7 | 4.10 | 2.21 |
| 130 | 14.2 | 3.43 | 2.33 |
| 140 | 13.9 | 4.64 | 2.25 |
| 150 | 14.0 | 4.13 | 2.27 |
| 160 | 14.5 | 4.95 | 2.41 |
| 170 | 14.2 | 5.53 | 2.31 |
| 180 | 14.7 | 6.31 | 2.40 |
| 190 | 14.5 | 5.56 | 2.36 |
| 200 | 14.2 | 5.92 | 2.29 |
| 210 | 14.5 | 6.04 | 2.36 |
| 220 | 14.5 | 5.84 | 2.34 |
| 230 | 14.5 | 5.14 | 2.27 |
| 240 | 14.7 | 6.95 | 2.33 |
| 250 | 14.7 | 5.88 | 2.32 |
| 260 | 14.7 | 5.48 | 2.34 |
| 270 | 14.2 | 5.12 | 2.16 |
| 280 | 14.5 | 5.34 | 2.23 |
| 290 | 14.8 | 5.68 | 2.30 |
| 300 | 14.4 | 4.49 | 2.14 |
| 310 | 15.1 | 5.70 | 2.30 |
| 320 | 14.9 | 6.47 | 2.27 |
| 330 | 15.0 | 5.78 | 2.32 |
| 340 | 14.7 | 5.52 | 2.19 |
| 350 | 14.7 | 4.62 | 2.19 |
| 375 | 15.2 | 5.87 | 2.31 |
| 450 | 16.0 | 4.70 | 2.52 |
| 500 | 18.4 | 3.46 | 3.11 |
| 525 | 16.8 | 3.78 | 2.65 |
| 550 | 18.4 | 3.46 | 3.11 |

## References


[1] X. Dong, K. Lin, C. Yu, W. Zhang, W. Li, Q. Zhang, Q. Zhang, J. Liu, Y. Cao, X. Xing, *Scripta. Mater.* **2023**, *229*, 115388.

[2] Y. Song, J. Chen, X. Liu, C. Wang, J. Zhang, H. Liu, H. Zhu, L. Hu, K. Lin, S. Zhang, X. Xing, *J. Am. Chem. Soc.* **2018**, *140*, 602.

[3] Lin, W. Zhang, C. Yu, Q. Sun, Y. Cao, W. Li, S. Jiang, Q. Li, Q. Zhang, K. An, Y. Chen, D. Yu, J. Liu, K. Kato, Q. Zhang, L. Gu, X. Kuang, Y. Tang, J. Miao, X. Xing, *Cell. Rep. Phys. Sci.* **2023**, *4*, 101254.

[4] Y. Cao, Y. Xu, S. Khmelevskyi, M. Avdeev, C.-W. Wang, S. Hu, K. Ohara, Y. Xia, X. Chen, Q. Li, J. Deng, J. Miao, K. Lin, X. Xing, *Chem. Mater*. **2023**, *35*, 9167.

[5] W. Li, K. Lin, Y. Yan, C. Yu, Y. Cao, X. Chen, C. W. Wang, K. Kato, Y. Chen, K. An, Q. Zhang, L. Gu, Q. Li, J. Deng, X. Xing, *Adv. Mater.* **2022**, *34*, 2109592.

[6] C.-E. Guillaume, *Compt. Rend*. **1897**, *125*, 235.

[7] A. E. Phillips, G. J. Halder, K. W. Chapman, A. L. Goodwin, C. J. Kepert, *J. Am. Chem. Soc.* **2010**, *132*, 10.

[8] C. Yu, K. Lin, X. Chen, S. Jiang, Y. Cao, W. Li, L. Chen, K. An, Y. Chen, D. Yu, K. Kato, Q. Zhang, L. Gu, L. You, X. Kuang, H. Wu, Q. Li, J. Deng, X. Xing, *Nat. Commun*. **2023**, *14*, 3135.

[9] Y. Sun, Y. Cao, S. Hu, M. Avdeev, C.-W. Wang, S. Khmelevskyi, Y. Ren, S. H. Lapidus, X. Chen, Q. Li, J. Deng, J. Miao, K. Lin, X. Kuang, X. Xing, *J. Am. Chem. Soc.* **2023**, *145*, 17096.

[10] Y. Song, Q. Sun, T. Yokoyama, H. Zhu, Q. Li, R. Huang, Y. Ren, Q. Huang, X. Xing, J. Chen, *J Phys Chem Lett* **2020**, *11*, 1954.

[11] Y. Sun, R. Yu, S. Khmelevskyi, K. Kato, Y. Cao, S. Hu, M. Avdeev, C. W. Wang, C. Yu, Q. Li, K. Lin, X. Kuang, X. Xing, *Nati. Sci. Rev.* **2025**, *12*, nwae462.